

Motion Planning for Physical Contact-based Interaction with a Flapping-wing Drone

Kazuki Numazato¹ and Moju Zhao²

Abstract—Flapping-wing drones have attracted significant attention due to their biomimetic flight, with numerous studies focusing on their wing structure and control methods. Compared to propeller-driven drones, flapping-wing drones are considered more human-friendly, making them suitable for human-drone interactions. However, few studies have explored the practical interaction between humans and flapping-wing drones. In this study, we propose an interaction system in which a flapping-wing drone performs a perching motion on a human hand. To achieve a safe approach toward humans, we design a trajectory planning method that considers both physical and psychological human factors. We implement this trajectory and conduct experiments to evaluate the system's performance, including success rate and user perception. The results demonstrate that our approach enables safe and effective perching interactions. To the best of our knowledge, this study is the first to investigate physical contact interactions between humans and flapping-wing drones.

I. INTRODUCTION

In recent years, extensive research has been conducted on Human-Drone Interaction (HDI), exploring various applications. In particular, physical contact-based interaction between drones and humans has gained increasing attention, as it has the potential to expand the scope of drone applications such as [1], [2]. However, ensuring physical and psychological safety during physical contact has been a significant challenge, especially when using conventional propeller-driven drones. The rapid rotation of propellers poses a potential risk of injury, making it difficult to design safe and natural interactions. Additionally, the high-frequency noise and mechanical appearance of propeller drones often induce psychological discomfort, further limiting their acceptance in close human proximity[3], [4] . To address these issues, previous studies have made proposals such as safeguard mechanisms to cover the drone body[4], [5], drones that has an familiar appearance to human[4], emotion encoding[6], and bio-inspired propellers that make less noise[7].

In contrast, flapping-wing drones, inspired by the flight of birds and insects, offer several inherent advantages that make them particularly suitable for physical contact-based interaction[8]. First, the soft and oscillatory motion of the wings minimizes the physical impact during contact, greatly enhancing physical safety. Second, flapping-wing

drones produce more natural sound compared to propeller-driven drones, reducing psychological discomfort during interaction. Third, the biomimetic appearance and motion of flapping-wing drones evoke a sense of familiarity and warmth, promoting more natural and engaging human-drone interaction.

Despite these promising characteristics, most existing research on flapping-wing drones has primarily focused on their memchanical characteristics such as aerodynamics, wing design, and flight control[9], [10], [11], with little attention given to research on the methodology for them to interact with humans in a physically and psychologically safe way, especially in scenarios involving direct physical contact. To the best of our knowledge, no prior study has specifically investigated the design and implementation of physical contact-based interaction system using flapping-wing drones. This presents a significant research gap in leveraging the unique properties of flapping-wing drones to enhance the quality of human-drone interaction.

Thus, in this study, we propose an interaction system in which a flapping-wing drone performs a palm landing motion on a human hand, enabling direct physical contact in a safe and natural manner. To achieve this, we design a trajectory planning method that considers both physical and psychological human factors to facilitate safe and comfortable approaches. We implement this method on a flapping-wing drone and conduct real-world experiments to evaluate its palm landing success rate and valiability.

We focus on palm landing because enabling palm landing has several potential advantages described as follows.

- 1) It allows environment-adaptive interaction. In crowded or spatially constrained environments, landing on a fixed surface is often impractical. However, by utilizing the human body as a dynamic landing platform, the drone can overcome spatial limitations and operate more flexibly. This approach is particularly useful in urban scenarios, public transportation, or remote field operations.
- 2) It contributes to energy efficiency enhancement. Drones have limited battery capacity and typically consume significant energy when hovering. By landing on a human palm during idle periods, the drone can conserve energy and extend its operational time. This energy-efficient operation is critical for long-term service tasks, search and rescue missions, or continuous monitoring operations.
- 3) palm landing enhances personalized companion interaction. By physically landing on a human palm, a

*This work was not supported by any organization

¹Kazuki Numazato is with Faculty of Electrical Engineering, Mathematics and Computer Science, University of Twente, 7500 AE Enschede, The Netherlands albert.author@papercept.net

²Bernard D. Researcheris with the Department of Electrical Engineering, Wright State University, Dayton, OH 45435, USA b.d.researcher@ieee.org

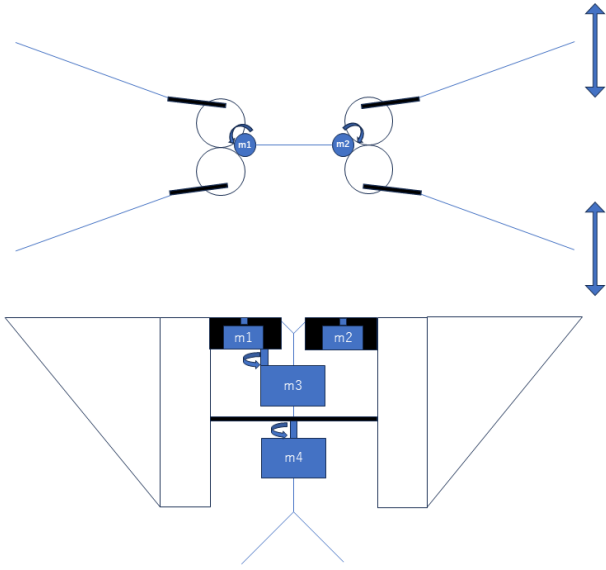


Fig. 1: The mechanical structure model of a flapping-wing drone. It has motors for thrust (m_1, m_2), a motor for wing orientation (m_3), and a motor for yaw control (m_4).

drone can provide pet-like interaction, evoke emotional attachment, or facilitate social engagement. This is particularly promising for children, the elderly, or individuals with social isolation, where physical interaction fosters a stronger sense of companionship.

These advantages highlight the potential of palm landing as a key interaction modality for flapping-wing drones, enabling a wide range of applications in various scenarios.

The main contributions of this work can be summarized as follows:

- 1) We propose a human-friendly interaction system utilizing a flapping-wing drone, focusing on trajectory planning.
- 2) We develop an intuitive device system for drone interaction.
- 3) We verify the proposed model using an actual drone.

The remainder of this paper is organized as follows. The basic mechanical characteristics and control method of flapping-wing drone is introduced in Section II. The motion planning based on physical and psychological factors is presented in Section III, followed by the experimental results in Section V before concluding in Section VI.

II. MODELING

In this section, we describe the dynamic model and control of a basic flapping-wing drone.

A. Dynamic Model

Based on the model depicted in Fig. 1, the three-dimensional force f_i generated by m_i can be written as:

$$\{CoG\} \mathbf{f}_i = \lambda_i \{CoG\} \mathbf{u}_i, \quad (1)$$

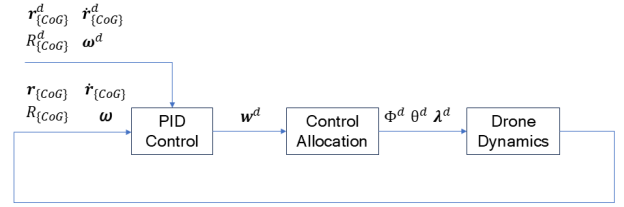


Fig. 2: The PID control model of a flapping-wing drone. It has mot

$$\{CoG\} \mathbf{u}_i = \{CoG\} R_{\{F_i\}}(\phi_i, \theta_i) \begin{bmatrix} 0 \\ 0 \\ 1 \end{bmatrix}, \quad (2)$$

where $\{CoG\} R_{\{F_i\}}(q, \phi_i, \theta_i)$ is the rotation matrix of the motor frame $\{F_i\}$ w.r.t. the frame $\{CoG\}$, and λ_i is the thrust coefficient of the m_i . ϕ_i and θ_i are rotational angles of the m_3 and m_4 , respectively. The total force and torque generated by m_1 and m_2 can be written as:

$$\begin{bmatrix} \{CoG\} \mathbf{f}_\lambda \\ \{CoG\} \boldsymbol{\tau}_\lambda \end{bmatrix} = \begin{bmatrix} \sum_{i=1}^2 \{CoG\} \mathbf{f}_i \\ \sum_{i=1}^2 \{CoG\} \mathbf{p}_i \times \{CoG\} \mathbf{f}_i \end{bmatrix} = Q \boldsymbol{\lambda}, \quad (3)$$

$$Q = \begin{bmatrix} \{CoG\} \mathbf{u}_1 & \{CoG\} \mathbf{u}_2 \\ \{CoG\} \mathbf{p}_1 \times \{CoG\} \mathbf{u}_1 & \{CoG\} \mathbf{p}_2 \times \{CoG\} \mathbf{u}_2 \end{bmatrix} \quad \boldsymbol{\lambda} = [\lambda_1 \quad \lambda_2]^T. \quad (4)$$

The whole dynamic model can be written as follows:

$$m^{\{W\}} \ddot{\mathbf{r}}_{CoG} = \{W\} R_{\{CoG\}} \mathbf{f}_\lambda - m\mathbf{g} + \sum_{i=1}^{N_c} \{W\} \mathbf{f}_{c_i}, \quad (5)$$

$$I\dot{\boldsymbol{\omega}} + \boldsymbol{\omega} \times I\boldsymbol{\omega} = \boldsymbol{\tau}_\lambda + \sum_{i=1}^{N_c} \{CoG\} \mathbf{p}_{c_i} \times \{W\} R_{\{CoG\}}^T \{W\} \mathbf{f}_{c_i}, \quad (6)$$

where m is the mass of the drone, I is the inertia matrix, \mathbf{r}_{CoG} is the position of the center of gravity, \mathbf{g} is the gravity vector, \mathbf{f}_{c_i} is the contact force, and \mathbf{p}_{c_i} is the position of the contact point.

B. Control

The control model of the flapping-wing drone is shown in Fig. 2. Based on the dynamics of (5) and (6), we can design a PID controller for the flapping-wing drone. One of the control inputs is the desired force \mathbf{f}_λ^d , which can be written as:

$$\begin{aligned} \{CoG\} \mathbf{f}_\lambda^d = & m^{\{W\}} R_{\{CoG\}}^T \left(K_{f,p} \mathbf{e}_r + K_{f,i} \int \mathbf{e}_r dt + K_{f,d} \dot{\mathbf{e}}_r \right) \\ & + \{W\} R_{\{CoG\}}^T \left(m\mathbf{g} - \sum_{i=1}^{N_c} \{W\} \mathbf{f}_{c_i} \right). \end{aligned} \quad (7)$$

where $K_{f,*}$, are the PID gain diagonal matrices, and $\mathbf{e}_r = \{{}^W\}\mathbf{r}_{\{CoG\}}^d - \{{}^W\}\mathbf{r}_{\{CoG\}}$ is the position error.

The attitude control follows the part of the control method proposed by [12]:

$$\begin{aligned} \{{}^{CoG}\}\boldsymbol{\tau}_{\lambda}^d &= I \left(K_{\tau,p} \mathbf{e}_R + K_{\tau,i} \int \mathbf{e}_R dt + K_{\tau,d} \mathbf{e}_{\omega} \right) \\ &\quad + \boldsymbol{\omega} \times I\boldsymbol{\omega} - \sum_{i=1}^{N_c} \mathbf{p}_{c_i} \times R^T \mathbf{f}_{c_i}, \end{aligned} \quad (8)$$

$$\mathbf{e}_R = \frac{1}{2} (R^T R^d - (R^d)^T R)^{\vee}, \quad (9)$$

$$\mathbf{e}_{\omega} = R^T R^d \boldsymbol{\omega}^d - \boldsymbol{\omega}. \quad (10)$$

where $[{}^*]^\vee$ is the inverse of a skew map, and $R := \{{}^W\}R_{\{CoG\}}$ for convenience. Then, the desired wrench w.r.t the frame $\{CoG\}$ can be summarized as follows:

$$\mathbf{w}^d = [\{{}^{CoG}\}\mathbf{f}_{\lambda}^d \quad \{{}^{CoG}\}\boldsymbol{\tau}_{\lambda}^d]^T. \quad (11)$$

III. MOTION PLANNING

To design a motion planning method that minimizes psychological discomfort when a flapping drone approaches a human, we must consider the several factors:

A. Distance

Given the expected size and shape of a flapping drone, we estimate that the minimum acceptable distance falls within a specific range. By maintaining this distance while gradually invading the landing zone, the psychological burden can be minimized. Several studies have investigated the psychological burden imposed by drones depending on their distance from humans using different drone sizes[4], [13], [14], [15]. [13] is a paper focusing on tactile drone interaction using a drone with a wheelbase of 0.92m, which is suitable for palm landing. This paper conducted an experiment in which participants were asked to stop the drone when they felt uncomfortable by using foot (non-contact) and hand (contact) methods. The results show that the maximum stop distance was approximately 1.25m, which means that, if the drone needs to approach closer than this distance, it should be done in psychologically safe manners such as gradually decreasing the speed or using a trajectory that does not directly approach the user so that the user does not feel threatened.

Moreover, the study [13] also shows that even the minimum stop distance was above 0.30m, which means that the drone should not approach the user closer than this distance. This indicates that physical contact should occur outside this range to guarantee physical and psychological safety.

B. Altitude

In the study [13], the height was set to enable a convenient way of tactile interaction by allowing the participants to slightly look down to the quadrotor. We follow this setting because then users do not need to move their head to look up to the drone and are able to simultaneously observe both the

drone and their own hand, which leads to easier adjustments of the hand position while the drone is approaching. Assuming that users lift their hand to the height of their elbow for palm landing, the drone should be positioned at the height of between the elbow and the eye level.

C. Approach Direction

As noted in [13], the approach direction of the drone affects the psychological burden. The study shows that the participants felt most uncomfortable when the drone approached them from the back because they could not see the drone. Therefore, the drone should approach the user from the front or side to minimize the psychological burden.

D. Velocity

To assess the appropriate velocity of the drone, we need to consider the human perception of speed of an approaching object. The study [16] shows that the drivers' perception of the speed of an foregoing vehicle follows Weber's Law:

$$k \frac{\Delta W}{W} = \Delta s \quad (12)$$

where W is the measurable stimuli, s the intensity of sensation, Δ the increment of physical quantity (W) and sensation intensity (s), and k the coefficient. In the study [16], W corresponds to the the distance between the cars and s to the speed of the driver's car. We assume that the same law can be applied to the perception of the speed of an approaching drone by regarding the distance between the drone and the user as W and the perceptive speed of the drone as s . This assumption explains the result of the previous study on perceived safety of drones [17], which shows the trend that larger distances are perceived as overly safe while a fast-moving drone close to participants is perceived as less safe than needed, because we can consider from the law that the participants perceive the speed of the drone as too slow due to the large distance between the drone and the participants and as too fast due to the short distance between the drone and the participants. Denoting the speed of the drone as v , the distance between the drone and the user as d , and time as t , we can derive the following equation:

$$k \frac{v \Delta t}{d} = \Delta s \quad (13)$$

To secure the psychological safety, the drone should approach the user keeping Δs constant. Thus, the speed can be calculated as follows:

$$v = \frac{k' d}{\Delta t} \quad (14)$$

where k' is a constant. We let $k' = 0.2$ in the present study.

E. Trajectory Design

Based on the above findings, we propose the following motion planning method, as illustrated in Figure 3. We divide the approach trajectory into four domains based on the distance between the drone and the user r .

- 1) $r > r_v$

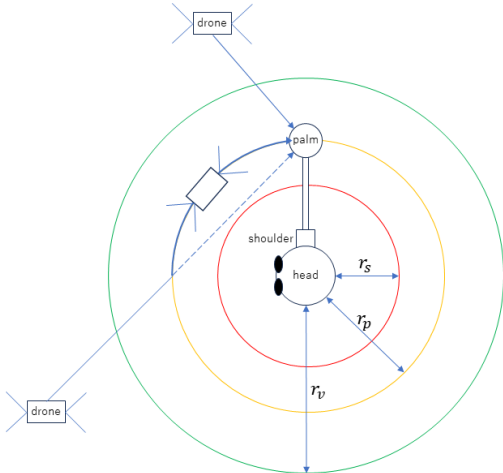


Fig. 3: Proposed motion planning for flapping drone approach. It has 4 domains which are separated by the distance from the user. Different strategies are applied to drone motion in different domains.

The drone is far from the user and approaches the palm straight at a constant speed. We let $r_v = 1.25$ based on III-A.

2) $r_v \geq r > r_p$

The drone is close enough to the user to be possibly perceived as unsafe, so it gradually decreases its speed by following (14).

3) $r_p \geq r > r_s$

The drone is inside the circle with the radius of user's arm length r_p centered at the user's chest. To maintain a certain distance from the user, the drone moves along the circle toward the user's palm while decelerating. On this path, the velocity of the drone towards the user's chest is always zero, which means $\Delta s = 0$ in (14) and minimizes the threat to the perceived safety.

4) $r \leq r_s$

If the drone is within this range, it is too close to the user and has a high risk of collision. Thus, the drone avoids the user by moving away from the user's body. Moreover, if the palm is within this range, the drone stays still and waits for the user to move their palm to the landing position outside the range so that the drone will not intrude the domain. We let $r_s = 0.30m$ based on III-A.

IV. EXPERIMENT

In this section, we first describe the testbed and then present the results of the experiments.

A. Testbed

1) *Overall system:* Fig. 4 illustrates the overall experimental system configuration. The system consists of a motion capture (MoCap) system, a flapping-wing drone, a

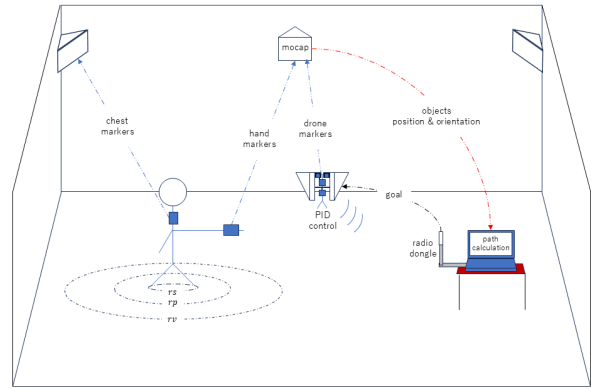


Fig. 4: Overall system configuration.

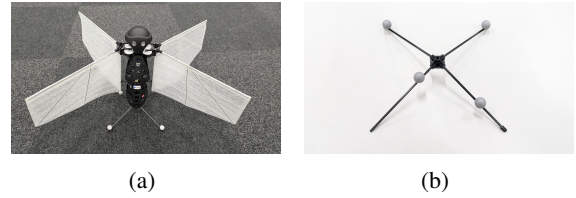


Fig. 5: Flapper Nimble+ drone (a) and its leg with motion capture markers (b).

user wearing devices, and a PC for trajectory planning and control. The MoCap system tracks the 3D positions and orientations of the user's chest, palm, and the drone in real time. We place 8 Optitrack Prime 13 cameras on the 4 corners and 4 sides of the room. The user wears chest-mounted and wrist-mounted markers allowing the system to capture intuitive control gestures. The PC processes the positional data and calculates the drone's optimal approach path toward the user's palm while maintaining a safe distance. The computed path is transmitted to the drone via a radio dongle, ensuring real-time control. The drone goes to the newest goal received from the PC using PID control, adjusting its motion dynamically based on feedback from the MoCap system.

Then, we describe the drone used in the experiment and the interface for control in detail.

2) *Flapping Drone:* Flapper Nimble+ used in the experiment, shown in (5a), is a bioinspired flapping-wing drone by FLAPPER DRONES compatible with the Crazyflie software, which is an open-source platform for research and development of quadcopters produced by Bitcraze AB. As shown in 5b attached four motion capture markers on its legs for tracking its position and orientation.

3) *Interface For Control:* As noted in III-3, the drone has to change its behavior according to the position of the user's palm. To facilitate intuitive control, we designed a wearable interface consisting of:

- A chest-mounted device shown in (6a)
- A wrist-mounted device shown in (6b)

Both devices were fabricated using a Bambu Lab X1-Carbon 3D printer. With these devices, we acquire the user's

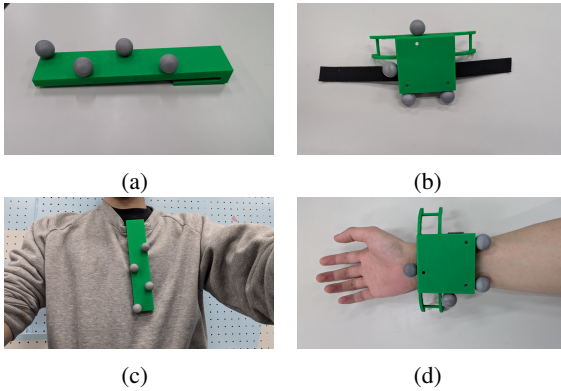


Fig. 6: Chest-mounted device (a) and wrist-mounted device (b) for controlling the state of flapping drone. The devices are attached to the user’s body as illustrated in (c, d).

palm position and orientation from the motion capture system and calculate the desired drone behavior based on the user’s palm position. This interaction design only requires arm bending and stretching to switch the state of the drone and thus enables a seamless and intuitive approach control.

B. Results and Analysis

1) *Trajectory Mapping*: We mapped the actual flight trajectories of the drone in both 2D and 3D and compared them with the planned trajectory proposed in Section 3.

2) *Velocity Profile*: We analyzed the velocity profile of the drone to examine:

- The presence or absence of overshoot.
- Whether the approach was perpendicular to the user’s palm.

3) *Success Rate Analysis*: The success rate of the system was evaluated by measuring the number of successful trials over multiple attempts. This metric was used to assess the reproducibility and reliability of the system.

4) *Distance Between Chest and Drone*: A distance-time graph was generated to verify whether the drone maintained a safe distance from the user during the experiment.

V. CONCLUSIONS

A conclusion section is not required. Although a conclusion may review the main points of the paper, do not replicate the abstract as the conclusion. A conclusion might elaborate on the importance of the work or suggest applications and extensions.

APPENDIX

Appendices should appear before the acknowledgment.

ACKNOWLEDGMENT

The preferred spelling of the word acknowledgment in America is without an e after the g. Avoid the stilted expression, One of us (R. B. G.) thanks ... Instead, try R. B. G. thanks. Put sponsor acknowledgments in the unnumbered footnote on the first page.

References are important to the reader; therefore, each citation must be complete and correct. If at all possible, references should be commonly available publications.

REFERENCES

- [1] Pascal Knierim, Thomas Kosch, Valentin Schwind, Markus Funk, Francisco Kiss, Stefan Schneegass, and Niels Henze. Tactile drones - providing immersive tactile feedback in virtual reality through quadcopters. In *Proceedings of the 2017 CHI Conference Extended Abstracts on Human Factors in Computing Systems*, CHI EA ’17, p. 433–436, New York, NY, USA, 2017. Association for Computing Machinery.
- [2] Kei Nitta, Keita Higuchi, and Jun Rekimoto. Hoverball: augmented sports with a flying ball. In *Proceedings of the 5th Augmented Human International Conference*, AH ’14, New York, NY, USA, 2014. Association for Computing Machinery.
- [3] Beat Schäffer, Reto Pieren, Kurt Heutschi, Jean Marc Wunderli, and Stefan Becker. Drone noise emission characteristics and noise effects on humans—a systematic review. *International journal of environmental research and public health*, Vol. 18, No. 11, p. 5940, 2021.
- [4] Alexander Yeh, Photchara Ratsamee, Kiyoshi Kiyokawa, Yuki Uranishi, Tomohiro Mashita, Haruo Takemura, Morten Fjeld, and Mohammad Obaid. Exploring proxemics for human-drone interaction. In *Proceedings of the 5th International Conference on Human Agent Interaction*, HAI ’17, p. 81–88, New York, NY, USA, 2017. Association for Computing Machinery.
- [5] Parastoo Abtahi, David Y. Zhao, Jane L. E., and James A. Landay. Drone near me: Exploring touch-based human-drone interaction. *Proc. ACM Interact. Mob. Wearable Ubiquitous Technol.*, Vol. 1, No. 3, September 2017.
- [6] Jessica R. Cauchard, Kevin Y. Zhai, Marco Spadafora, and James A. Landay. Emotion encoding in human-drone interaction. In *2016 11th ACM/IEEE International Conference on Human-Robot Interaction (HRI)*, pp. 263–270, 2016.
- [7] Ryusuke Noda, Toshiyuki Nakata, Teruaki Ikeda, Di Chen, Yuma Yoshinaga, Kenta Ishibashi, Chen Rao, and Hao Liu. Development of bio-inspired low-noise propeller for a drone. *Journal of Robotics and Mechatronics*, Vol. 30, No. 3, pp. 337–343, 2018.
- [8] Guido de Croon. Flapping wing drones show off their skills. *Science Robotics*, Vol. 5, No. 44, p. eabd0233, 2020.
- [9] Ethan Billingsley, Mehdi Ghommeh, Rui Vasconcellos, and Abdessatar Abdelkefi. On the aerodynamic analysis and conceptual design of bioinspired multi-flapping-wing drones. *Drones*, Vol. 5, No. 3, p. 64, 2021.
- [10] Hala Rifai, Nicolas Marchand, and Guylaine Poulin. Bounded control of a flapping wing micro drone in three dimensions. In *2008 IEEE International Conference on Robotics and Automation*, pp. 164–169. IEEE, 2008.
- [11] Yao-Wei Chin, Jia Ming Kok, Yong-Qiang Zhu, Woei-Leong Chan, Javaan S Chahl, Boo Cheong Khoo, and Gih-Keong Lau. Efficient flapping wing drone arrests high-speed flight using post-stall soaring. *Science Robotics*, Vol. 5, No. 44, p. eaba2386, 2020.
- [12] Taeyoung Lee, Melvin Leok, and N Harris McClamroch. Geometric tracking control of a quadrotor uav on se (3). In *49th IEEE conference on decision and control (CDC)*, pp. 5420–5425. IEEE, 2010.
- [13] Marc Lieser, Ulrich Schwanecke, and Jörg Berdux. Evaluating distances in tactile human-drone interaction. In *2021 30th IEEE International Conference on Robot & Human Interactive Communication (RO-MAN)*, pp. 1275–1282. IEEE, 2021.
- [14] Brittany A. Duncan and Robin R. Murphy. Comfortable approach distance with small unmanned aerial vehicles. In *2013 IEEE RO-MAN*, pp. 786–792, 2013.
- [15] Urja Acharya, Alisha Bevins, and Brittany A. Duncan. Investigation of human-robot comfort with a small unmanned aerial vehicle compared to a ground robot. In *2017 IEEE/RSJ International Conference on Intelligent Robots and Systems (IROS)*, pp. 2758–2765, 2017.
- [16] Tasuku Takagi, Masanari Taniguchi, and Shosuke Suzuki. Weber-fechner law in road traffic flow. In *2012 Proceedings of SICE Annual Conference (SICE)*, pp. 1056–1061, 2012.
- [17] Sanne Van Waveren, Rasmus Rudling, Iolanda Leite, Patric Jensfelt, and Christian Pek. Increasing perceived safety in motion planning for human-drone interaction. In *Proceedings of the 2023 ACM/IEEE*

international conference on human-robot interaction, pp. 446–455,
2023.